

Verification of Effectiveness of a Matrix Converter with Boost-up AC Chopper by Using an IPM Motor

Kazuhiro Koiwa

Electrical, Electronics and Information Engineering
Nagaoka University of Technology
Nagaoka, Japan
newkoiwa@stn.nagaokaut.ac.jp

Jun-ichi Itoh

Electrical, Electronics and Information Engineering
Nagaoka University of Technology
Nagaoka, Japan
itoh@vos.nagaokaut.ac.jp

Abstract— This paper describes the matrix converter that features boost-up functionality. The proposed circuit topology connects a V-connection AC chopper at the input side of the matrix converter to achieve the boost-up function. The matrix converter and the V-connection AC chopper are controlled independently, where a virtual indirect control method is applied to the matrix converter, and an open-loop control is applied to the V-connection AC chopper. However, the efficiency of the proposed circuit is low due to the extra loss from the V-connection AC chopper. In this paper, the efficiency of the proposed circuit and the conventional matrix converter is evaluated by using a 3.7kW IPM motor in the simulation and the experiment. The simulation results confirm that by implementing field-weakening control in the conventional matrix converter, the losses are lower than that of the proposed circuit topology, where the proposed circuit improves the efficiency by 12%. According to the experimental results, it is obtained that the proposed circuit can improve the efficiency of 13% in compare with the conventional matrix converter.

I. INTRODUCTION

Matrix converters (MC) which can convert an AC power supply voltage directly into an AC output voltage of variable amplitude and frequency without the large energy storages, such as electrolytic capacitors, have been actively studied recently [1-15]. The following shows the advantages of the matrix converters comparing with the back-to-back converter system (BTB system), which is consist of a PWM rectifier and a PWM inverter; (i) light-weight and long-life due to no large passive components in the main circuit and (ii) high efficiency because of fewer switching devices are connected in the current path. The MC is expected to apply in the renewable energy field such as the hybrid electric vehicle systems, wind power generator systems and others.

However, the MC has a drawback in the voltage transfer ratio, which defines as the ratio between the output voltage and the input voltage, is being constrained to 0.866. Consequently, the output current of the MC is higher than that

of the BTB system, under the same output power. Even the motor can drive at rated frequency as the field-weakening control is applied. However, the output current is increased and the efficiency of the system is reduced. Further, the motor loss increases due to the high input motor current. Besides, the restricted voltage transfer ratio also limits the applications of the MCs.

There are many literatures which discuss on improving the voltage transfer ratio of the MCs. One of the easy solutions is to connect a transformer between the power supply and the MC. However, the commercial frequency transformer applies in the power grid frequency gives penalty in term of weight and size.

There are papers studied to apply over-modulation in the MC and successfully improved the voltage transfer ratio from 0.866 to 0.94 [13][14]. However, the input current and the output voltage contain large amount of harmonic components due to the square waveforms. Additionally, the amplitude of output voltage is lower than the input voltage. In other words, the MC cannot apply for the high voltage application. Therefore, in considering of applying the MC in the near future of power electronics fields, the boost-up functionality stands an important role.

On the other hand, a Matrix-Reactance Frequency Converter (MRFC), which consists of a MC and an AC chopper, has been studied in [12]. Reference [12] shows that, the amplitude of the output voltage can control to extend which is higher than the input voltage. However the MRFC requires many components due to the insertion of the boost up reactor and capacitor. In addition, the control becomes complicated due to the requirement of regular synchronizing between the MC and the chopper.

This paper demonstrates the matrix converter circuit topology which connects the V-connection AC chopper at the input side of the MC [3][15]. The additional component of this circuit is only consisting of the bi-directional switches because the reactors in the input filter are being used as boost-up reactors in this method. Also, the automatic voltage controller

(AVR) for the chopper is not required in this system. As a result, the value of the capacitor needed in the boost-stage is smaller than that of the DC capacitor in a BTB system. Moreover, the origin advantages of the MC remain in the proposed circuit because the V-connection AC chopper is ideal (no switching operation) when the output voltage is lower than the maximum value of the voltage transfer ratio (0.866). However, the proposed circuit has two problems such as following. At first, the input current distorts due to the input filter resonance. Secondary, in comparison with the conventional MC, the efficiency of the proposed circuit is degraded due to the chopper loss.

In this paper, the proposed circuit is simulated and experimented by using a 3.7kW-Interior Permanent Magnet motor (IPM motor). At first, in order to suppress the input filter resonance, the input current stability control is applied in the chopper. Secondary, in the simulation, the control applies with the field-weakening control, and compares the efficiency of the system by using the proposed circuit with the conventional MC. Finally, the validity of the simulation results will be confirmed by experiment.

II. CIRCUIT TOPOLOGY

Figure 1 shows the proposed circuit diagram. The proposed circuit connects a V-connection AC chopper at the input side of the MC. The additional components are based on eight IGBTs that are mainly constructed by silicon and diodes. The relationships between the input voltage v_{in} and the output voltage v_{out} is expressed by

$$v_{out} = \beta_{chop} \cdot \lambda_{mc} \cdot v_{in} \quad (1),$$

where, λ_{mc} is the modulation index of the MC, β_{chop} is the boost-up ratio of the chopper and v_{in} is the input voltage. The proposed circuit does not require a voltage control for the input capacitor. Therefore, the capacitor value does not dominant by the voltage control response and the current response for the input side. As a result, the V-connection AC chopper and the components do not dominate the size and the weight in comparison to the origin structure of a MC.

The maximum output voltage of the proposed circuit is decided by the duty ratio of the V-connection AC chopper. It should be noted that the switches in the V-connection AC chopper is ideal (no operation) when the voltage transfer ratio is lower than 0.866 of the input voltage. That is, at the range of low output voltage, the switching losses does not occur.

Besides, since the MC uses bi-directional switches, are required to apply with commutation pattern to prevent the source and load from open circuit and short circuit. In this paper, the 4-step commutation method is applied in the proposed circuit. Moreover, the voltage of the filter capacitors is used in this commutation [8].

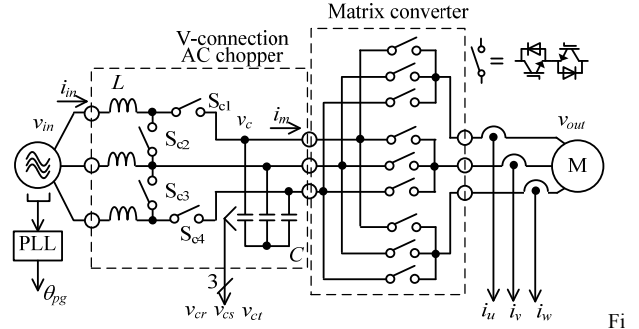


Figure 1. Circuit configuration of the proposed circuit.

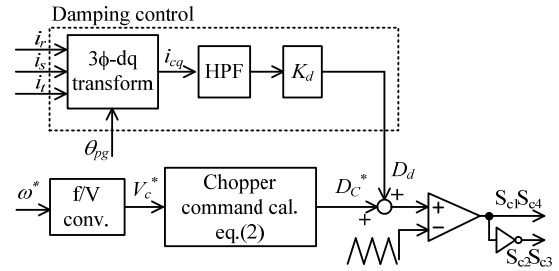


Figure 2. Control diagram in the chopper.

III. CONTROL STRATEGY

A. Boost-up Chopper Control

Figure 2 shows the control diagram in the chopper with the damping control. The voltage command D_c^* for the V-connection AC chopper is expressed by

$$D_c^* = \frac{\lambda_{mc}}{V_c^*} \quad (2),$$

where, V_c^* is the voltage command which is converted from the rotating speed command.

In order to suppress the oscillation in the input current from the resonance of the input filter, a stabilization control for the matrix converter has been proposed in Reference [5]-[6]. In these papers, the distortion component of the terminal voltage is removed by using a band pass filter (BPF). After that, the distortion components are subtracted by the input current command. In this paper, the input current stability control is applied to the chopper instead of the matrix converter. The damping control is implemented on the d-q frame of the AC chopper control. The fundamental frequency component on the d-q frame becomes a constant value, i.e. DC signal. In addition, the harmonics components are appeared as ripple components. The distortion component of the input current i_{dq} is extracted by using a high pass filter (HPF). After that, the distortion component is added to the chopper command D_c^* .

The damping control operates for the distortion component as the feedback regulator. On the other hand, the fundamental component is not affected. For this reason, the chopper control does not require the high speed response [10]. It means that the filter capacitor and the boost-up reactor are not dominated

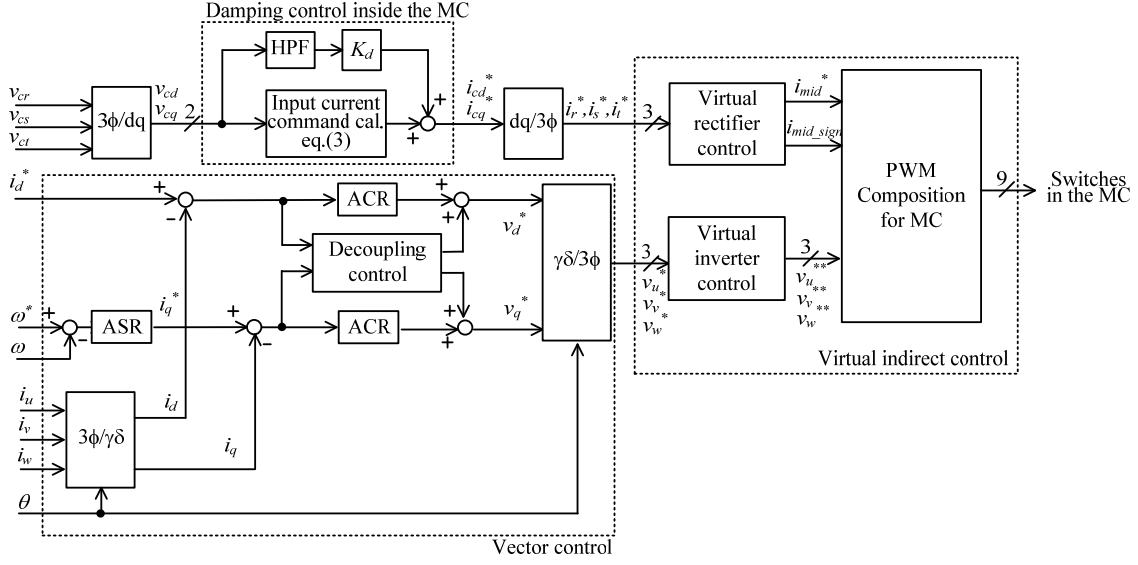


Figure 3. Control block diagram of the proposed circuit.

by the control response of the input current and the capacitor voltage.

B. Matrix Converter Control

Figure 3 shows the control block diagram of the MC. In this paper, the vector control is constructed from the ACR (Automatic Current Regulator) and the ASR (Automatic Speed Regulator). In addition, the pulse pattern of the MC is generated by the virtual indirect control method [2]. The input current command i_{cd}^* and i_{cq}^* are generated from the capacitor voltage [5]. Thus, they are expressed by (3) and (4), respectively.

$$i_{cd}^* = \frac{p \cdot v_{cd} - q \cdot v_{cq}}{v_{cd}^2 + v_{cq}^2} \quad (3)$$

$$i_{cq}^* = \frac{p \cdot v_{cq} - q \cdot v_{cd}}{v_{cd}^2 + v_{cq}^2} \quad (4)$$

where, p is the active power command, q is the reactive power command.

Figure 4 shows the vector control block diagram of the MC. Figure 4-(a) and 4-(b) show the control block diagram of ACR and ASR, respectively. The transfer function of the ACR and the ASR are expressed by (5) and (6), respectively.

$$G_{ACR} = \frac{I}{I^*} = \frac{\frac{K_I}{T_I L_a}}{s^2 + \frac{R_a + K_I}{L_a} s + \frac{K_I}{T_I L_a}} \quad (5)$$

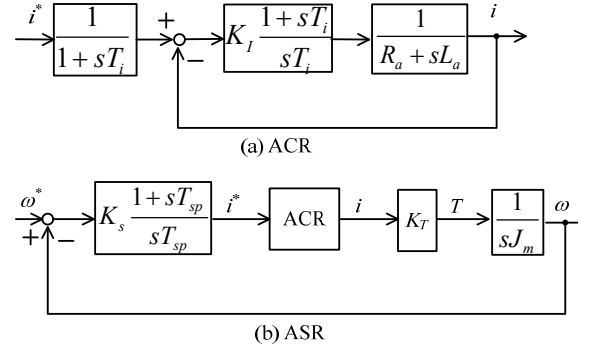


Figure 4. Vector control diagram of the MC.

$$G_{ASR} = \frac{\omega}{\omega^*} = \frac{\frac{K_{sp} K_T}{T_{sp} J_m}}{s^2 + \frac{K_{sp} K_T}{J_m} s + \frac{K_{sp} K_T}{T_{sp} J_m}} \quad (6)$$

where, the transient response of the ACR is faster than the ASR and the equation (6) is calculated by equaling the gain of the ACR to 1. Also, K_{sp} and T_{sp} are the proportional gain and the integrated time of the ASR, respectively. K_I and T_I are the proportional gain and the integrated time of ACR, respectively.

C. Field-weakening Control

Figure 5 shows the vector diagram of the field-weakening control where e_q is the back electromotive force, v and v' are the terminal voltage in the IPM motor without the field-weakening control and with the field-weakening control. Field-weakening control in the IPM motor can equally weaken the magnetic flux in the permanent magnet from the d axis armature magnetic flux. As a result, the rotation speed area can be extended by implementing the field-weakening control. From the figure 5, it is expressed by (7).

$$V_{om} = \sqrt{v_d^2 + v_q^2} \quad (7)$$

$$= \sqrt{(\omega L_q i_q)^2 + (\omega L_d i_d + e_q)^2}$$

where, V_{om} is the limited value of the output voltage. Therefore, d axis current is calculated by (8).

$$i_d = \frac{-\frac{e_q}{\omega} + \sqrt{\left(\frac{V_{om}}{\omega}\right)^2 - (L_q i_q)^2}}{L_d} \quad (8)$$

Table 1 shows the parameter of the IPM motor in this paper.

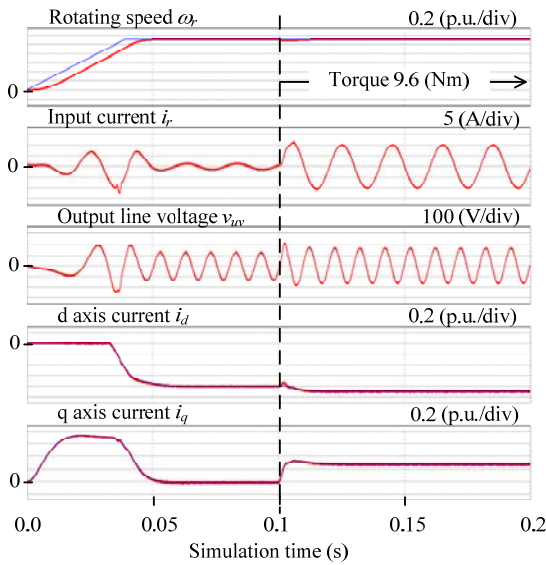
IV. SIMULATION AND EXPERIMENTAL RESULTS

A. Operation of the proposed circuit

Figure 6 shows the operation waveforms of the proposed circuit and the conventional MC (CMC). Table 2 provides the conditions for the simulation circuit and the experiment. The rotating speed, d and q axis current are standardized at the synchronous speed and the rated current, respectively. According to Figure 6-(a), it is confirmed that field-weakening control is applied in the MC at the high rotation speed area. On the other hand, in Figure 6-(b), the d-axis current shows that the field-weakening control is not applied in the high rotation speed. The torque occurred by the IPM motor is expressed by (9).

$$T = P_n [\psi_a i_q + (L_d - L_q) i_d i_q] \quad (9)$$

where, P_n is pole of the motor. In addition, ψ_a is the magnetic flux by the permanent magnet. According to this equation, the torque of the IPM motor is not only depended on the q-axis current but also the d-axis current. Thus, in Figure



(a) Conventional matrix converter.

6-(a), q-axis current is decreased in comparison with Figure 6-(b) due to the d-axis current. Besides, it is confirmed that the output voltage is higher in compared with the conventional MC.

Figure 7 shows the operation waveforms of the proposed circuit. Figure 7-(a) shows the operation waveform without applying the input current stability control method in the chopper. Then, the total harmonic distortion (THD) of the input current and output voltage THD are 18.9% and, 7% respectively. It is confirmed that the resonance distortion occur in the input current waveform. On the other hand,

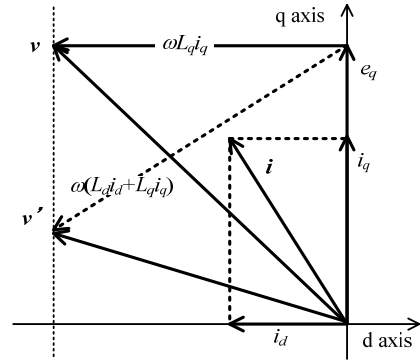
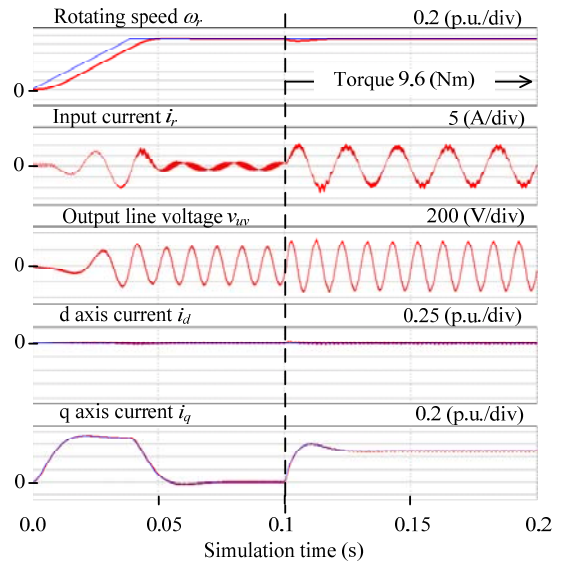


Figure 5. Phaser vector diagram on the field-weakening control.

TABLE 1 MOTOR PARAMETERS.

Rated power	3.7kW	Winding resistance R_c	0.693 Ω
Back Electromotive Force	151 V	d axis inductance L_d	6.2 mH
Rated current	14.2A	q axis inductance L_q	15.3 mH
Synchronous speed	1800 rpm	Inertia moment J_m	0.00255 kgm^2
Rated torque T_{eR}	19.6 Nm	Pole	6
Rated acceleration time T_R	0.028 s	Load	IPM motor



(b) Proposed circuit (240V).

Figure 6. Operation waveforms in the simulation result.

TABLE 2 SIMULATION PARAMETERS.

Input phase voltage	115 V	Input reactor	2 mH	
Input frequency	50 Hz	Filter capacitor	13.2 μ F	
Carrier frequency	Chopper	10 kHz	Voltage transfer ratio of MC	
	MC			
Output voltage	MC	173V	Load(simulation)	
	Proposed circuit	200 V or 240 V	Load(experiment)	
Response angular frequency ω	ACR	2000 rad/s	Damping factor ζ	
	ASR	200 rad/s		
Proportional gain	$K_{I,d}$	1.78	Integrated time	
	$K_{I,q}$	4.51		
	K_{sp}	6.86		
			ACR ASR	0.7
			$T_{i,d}$	0.672 ms
			$T_{i,q}$	0.694 ms
			T_{sp}	7 ms

TABLE 3 EXPERIMENTAL PARAMETERS.

Input phase voltage	115 V	Input reactor	2 mH	
Input frequency	50 Hz	Filter capacitor	13.2 μ F	
Carrier frequency	Chopper	10 kHz	Voltage transfer ratio of MC	
	MC			
Response angular frequency ω	ACR	2000 rad/s	Load	
	ASR	50 rad/s		
Proportional gain	$K_{I,d}$	1.67	Integrated time	
	$K_{I,q}$	4.12		
	K_{sp}	1.6		
			$T_{i,d}$	8.95 ms
			$T_{i,q}$	22.1 ms
			T_{sp}	28 ms

Figure 7-(b) shows the operation waveform, where the damping controls is applied in the AC chopper to suppress the resonant distortion. For these results, it is confirmed that the output voltage can increase to 27 V. Furthermore, the input current THD and output voltage THD can be improved to 7.8% and, 1% respectively.

Figure 8 shows the acceleration and deceleration tests for the IPM motor by using the proposed circuit. Table 3 shows the experimental parameters. In Figure 8(a), the AC chopper is operating while the rotating speed command ω^* is over 0.9pu because the voltage transfer ratio of the MC is started limiting from this period. In other words, the voltage transfer ratio of the system is increased by the AC chopper. According to Figure 8(a), it is confirmed that the input and q-axis current are not drastically changed due to operation of the AC chopper. Therefore, the proposed circuit can improve the output voltage continuously. On the other hand, according to the deceleration test shown Figure 8-(b), the IPM motor can be decelerated without large current from the input and q-axis current.

Figure 9 shows the experiment operation waveforms of the proposed circuit. Note that the proposed circuit operates the IPM motor in case of load torque equal to 20%. In other words, the mechanical power is equal to 720W. Additionally, the damping resistor and the damping control are not applied in the input filter and chopper. The resonant distortion in the input filter is suppressed due to the loss of the chopper. For this reason, the input current stability methods are applied in this prototype. According to Figure 9, it is confirmed that the voltage transfer ratio can be improved. The input current of the experiment is more distorted than that of the simulation. In the experimental, it is necessary to commute the switching

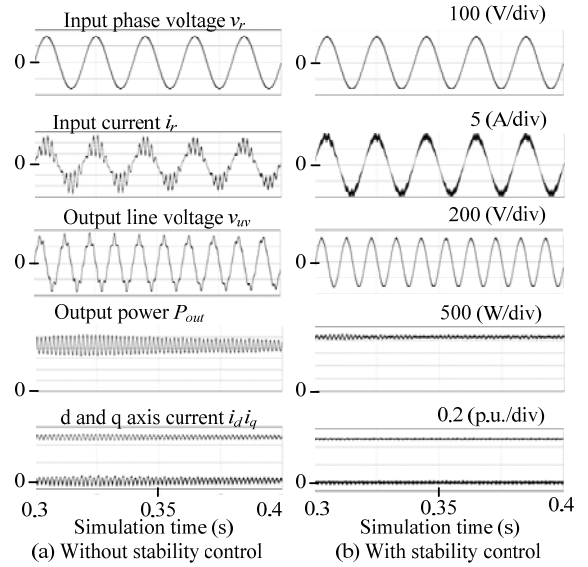


Figure 7. Effectiveness of stability control.

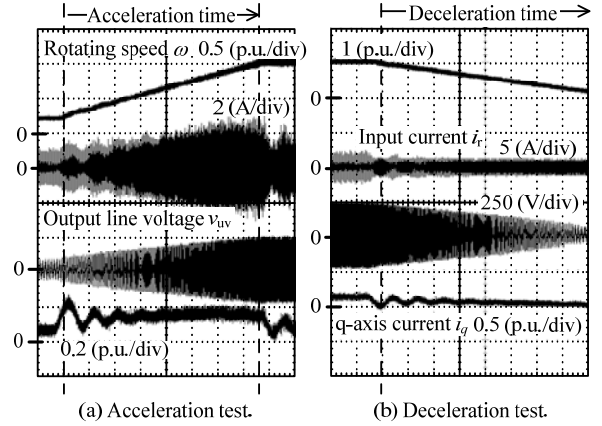


Figure 8. Acceleration and deceleration test of the IPM motor.

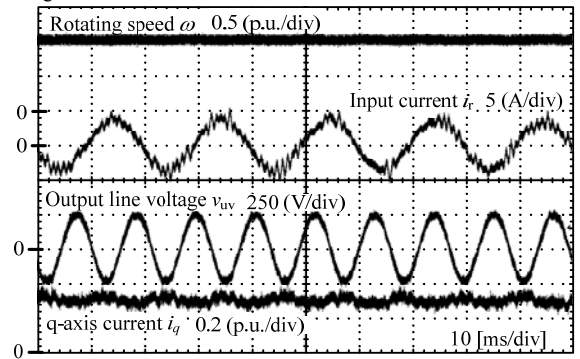


Figure 9. Steady operation test.

pattern to prevent the source and the load from short circuit or open circuit. As a result, the input current has distortions due to the voltage error which is caused by the switching commutation. Besides, there are commutation failures in the switching pattern because of the voltage detection error.

Figure 10 shows the total efficiency and the converter efficiency characteristics of the system by using the proposed circuit. It should be noted that the total efficiency is included the conversion efficiency and the motor efficiency. In addition,

the motor efficiency is calculated from the rotating speed and the detected torque. As a result, it is confirmed that the total efficiency and the converter efficiency at maximum point are 80.1% and 93.5% respectively.

Figure 11 shows the input and output current THD characteristics based on the mechanical power of the IPM motor. It is confirmed that the output current THD is less than 12%. On the other hand, the input current THD is less than 10%. The input current and output current THD becomes poor as the mechanical power reduces. This is because even the mechanical power reduces, although the harmonic distortion of the input and output current amplitude is constant, the fundamental amplitude of the input and output current becomes smaller.

B. Loss Analysis

Figure 12 is a simulation result shows the total efficiency characteristics [7]. The number in the column () in this figure shows the maximum voltage which is able to output by the converter. Note that the filter loss and the iron loss are not considered in this graph. In addition, the mechanical power is constantly equal to 2kW. The maximum efficiency of the proposed circuit is 91.1% at 1.11pu rotating speed. Thus, the efficiency of the proposed circuit is higher by 12% comparing with the conventional MC. The motor current in the conventional MC is increased due to the implementation of the field-weakening control. On the other hand, the motor current in the proposed circuit is not increased because the field-weakening control is not applied in the matrix converter. As a result, the efficiency of the proposed circuit is higher than that of the conventional MC.

Figure 13 is a simulation result shows the loss property. Note that the rotating speed is 1.11pu and the mechanical power is 2kW. According to this result, the loss of the proposed circuit is increased by the AC chopper. However, taken into consideration of the IPM motor loss, the loss of the proposed circuit is less than that of the conventional MC. This is because the copper loss of the IPM motor, the conduction loss of the Free Wheeling Diodes (FWD) and the conduction loss of the IGBTs are increased due to field-weakening control in the conventional MC.

Figure 14 shows the experimental efficiency comparison between the proposed circuit and the conventional MC. The torque is 12% and 20% in the experimental. However, the field-weakening control in the IPM motor is not capable of wide range of application. There, in order to extend the range of application, the input voltage of the proposed circuit and the conventional MC are degraded. As a result, high rotating speed of the IPM motor can be simulated. Accordingly, the total efficiency of the conventional MC which applied the field-weakening control becomes low as the input voltage decrease. This is because the conduction loss of the converter and the primary order copper loss of the IPM motor are increased to be larger due to the field-weakening control.

On the other hand, the AC chopper in the proposed circuit can improve the input voltage which has been decreased. Thus, the field-weakening control is not necessary to apply in the proposed circuit. For this reason, high efficiency of the

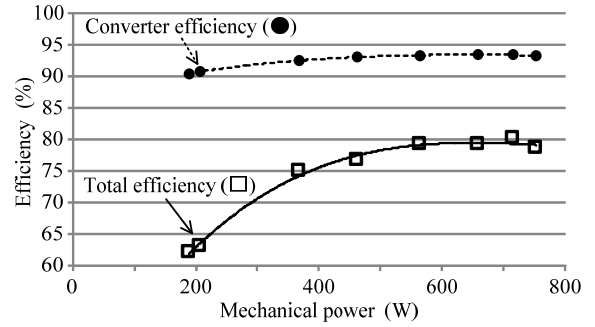


Figure 10. Efficiency characteristics of the proposed circuit.

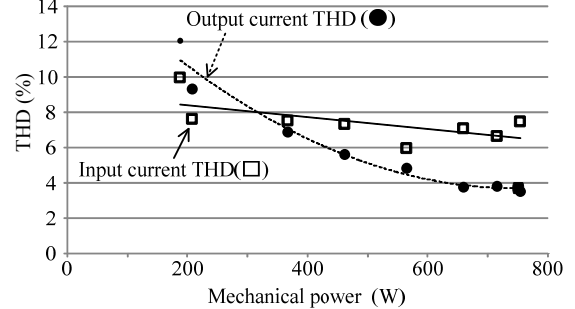


Figure 11. THD characteristics.

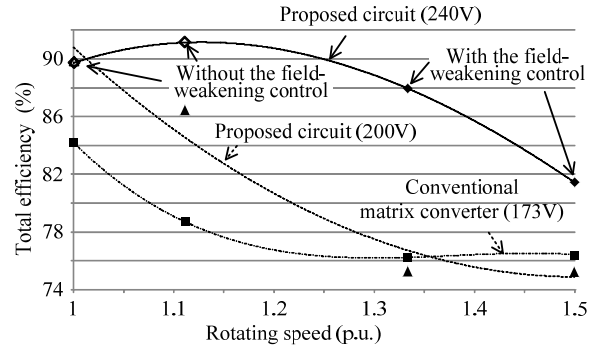


Figure 12. Total efficiency characteristics by the simulation result.

proposed circuit can be achieved. According to Figure 14, the efficiency of the proposed circuit can be improved by 13% in case of the input voltage is equal to 140V in comparing with the conventional MC. Therefore, high efficiency can be achieved without the field-weakening control and the validity of the simulation results are confirmed by experiment. Beside, when the rotating speed of engine generator is slow which results the supply voltage becomes low, the motor can efficiently to be driven, in order to implement the proposed circuit without the field-weakening control.

V. CONCLUSIONS AND FUTURE WORK

This paper discussed a circuit topology constructed from the MC and the V-connection AC chopper. The advantages of the proposed circuit are following;

- The proposed circuit has the advantages of the origin MC such as small size, light-weight and long life-time, even an AC chopper is added into the input side.

- The MC and the V-connection chopper can be controlled independently.

In this paper, the proposed circuit was modeled with a 3.7kW IPM motor in simulation and has proven the effectiveness of the proposed control. The simulation results confirmed that the proposed circuit could achieve a maximum efficiency of 91.1%. Additionally, the efficiency is shown by improving 12%. This is because the motor load current is increased due to the field-weakening control. Field-weakening control is applied at high rotating speed area that the converter fails to deliver high output voltage.

The proposed circuit was tested experimental by using the 3.7kW IPM motor. In the acceleration test, it is confirmed that the input and q-axis current are not drastically changed due to operation of the AC chopper. The proposed circuit achieves a unity input power factor and the voltage transfer ratio could be improved by the boost-up operation. The input current THD and output current THD are 7.5% and 3.53% respectively when the mechanical power is equal to 720W. The experimental results confirmed that the proposed circuit could achieve a maximum converter efficiency and total efficiency of 93.5 % and 80.1%, respectively. Therefore, the fundamental operation of the proposed circuit is confirmed by the experimental results. It was confirmed that the efficiency of system is affected by the field-weakening control in the experimental, where the input voltage decreases and the field-weakening control is implemented. As the result, the proposed circuit could improve the efficiency of 13% in case of the input voltage is equal to 140V in comparing with the conventional MC. Therefore, high efficiency of the drive system for the IPM motor could be achieved without the field-weakening control and the validity of the simulation results were confirmed by experiment.

In future works, the validity of these simulation results will be confirmed by using the IPM motor at the rated torque. Besides, in term of the converter and motor loss, the proposed circuit will compare with the BTB system.

REFERENCES

- [1] P. W. Wheeler, J. Rodriguez, J. C. Clare, L. Empringham: "Matrix Converters: A Technology Review" IEEE Transactions on Industry Electronics Vol. 49, No. 2, pp274-288, 2002.
- [2] J. Itoh, I. Sato, H. Ohguchi, K. Sato, A. Odaka and N. Eguchi: "A Control Method for the Matrix Converter Based on Virtual AC/DC/AC Conversion Using Carrier Comparison Method", IEEJ Trans., Vol.124-D, No.5, pp.457-463 (2004)
- [3] J.Itoh, K.Koiwa, K.Kato, "Input Current Stabilization Control of a Matrix Converter with Boost-up Functionality" International Power Electronics Conference 2010
- [4] Yasuhiro Tamai, Hideki Ohguchi, Ikuya Sato, Akihiro Odaka, Hironori Mine and Jun-ichi Itoh, "A Novel Control Strategy for Matrix Converters in Over-modulation Range," PCC NAGOYA 2007, pp. 1049-1055, Apr. 2-5 2007.
- [5] I. Sato, J. Itoh, H. Ohguchi, A. Odaka, and H. Mine: "An Improvement Method of Matrix Converter Drives Under Input Voltage Disturbances", IPEC-Niigata, pp. 546-551 (2005)
- [6] Junnosuke Haruna and Jun-ichi Itoh, "A Control Strategy for a Matrix Converter under a Large Impedance Power Supply," Power Electronics Specialists Conference 2007, pp. 659-664.
- [7] J. Itoh, T. Iida, A. Odaka: "Realization of High Efficiency AC link Converter System based on AC/AC Direct Conversion Techniques with RB-IGBT" Industrial Electronics Conference, Paris, PF-012149,2006
- [8] K. Kato, J. Itoh: "Development of a Novel Commutation Method which Drastically Suppresses Commutation Failure of a Matrix Converter," Trans.IEEJ,Vol.127-D,No.8,pp.829-836,2007
- [9] F. Schafmeister, C. Rytz and J. W. Kolar: "Analytical Calculation of the Conduction and Switching Losses of the Conventional Matrix Converter and the (Very) Sparse Matrix Converter", APEC 2005, pp.875-881, Vol.2
- [10] Zbigniew Fedyczak, Pawel Szczesniak, Igor Koroteyev; "New Family of Matrix-Reactance Frequency Converters Based on Unipolar PWM AC Matrix-Reactance Choppers" EPE-PEMC 2008, P170 pp.236-24
- [11] Zbigniew Fedyczak, Pawel Szczesniak, Marius Klytta; "Matrix-Reactance Frequency Converter Based on Buck-Boost Topology", EPE-PEMC 2006, pp.763-768
- [12] J. Itoh, H. Tajima, H. Ohsawa: "Induction Motor Drive System using V-connection AC Chopper", IEEJ Trans., Vol.123, No.3, pp.271-277 (2003)
- [13] Goh teck Chiang and J. Itoh: "Voltage Transfer Ratio Improvement of an Indirect Matrix Converter by Single Pulse Modulation", ECCE2010
- [14] Yasuhiro Tamai, Hideki Ohguchi, Ikuya Sato, Akihiro Odaka, Hironori Mine and Jun-ichi Itoh, "A Novel Control Strategy for Matrix Converters in Over-modulation Range," PCC NAGOYA 2007, pp. 1049-1055, Apr. 2-5 2007.
- [15] K. Koiwa, J. Itoh, "Experimental Verification for a Matrix Converter with a V-connection AC Chopper," EPE2011, pp. 1-10 (2011)

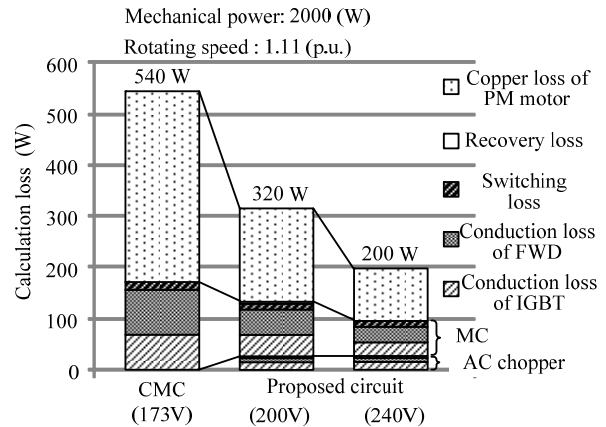


Figure 13. Property of the loss by simulation.

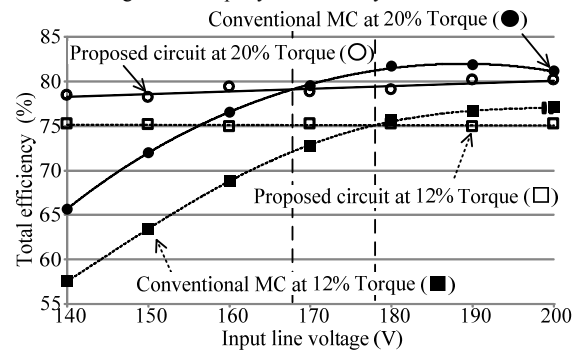


Figure 14. Efficiency comparison between the proposed circuit and the conventional MC by experiment.